Journal of Advance Research in Aeronautics and Space Science
Volume 7, Issue 1&2 - 2020, Pg. No. 1-14
Peer Reviewed Journal

Research Article

Unsteady Shock Interaction Mechanism on a Double Wedge at Mach 9

Sravan Kumar Kota[1], Sameer Ahamed Shaik[2], Rubens Talukder[3]

[1]Lead Design Engineer, [2]Chief Executive Officer, Department of Mechanical and Aeronautical, Samhams Technologies, Nellore, Andhra Pradesh, India.
[3]Chief Executive Officer, NexelT, Inc, Worldwide Corporate head Quarters, Canton, Michigan, USA.

I N F O

Corresponding Author:
Sravan Kumar Kota, Department of Mechanical and Aeronautical, Samhams Technologies, Nellore, Andhra Pradesh, India.
E-mail Id:
sravankumarkota88@gmail.com
Orcid Id:
https://orcid.org/0000-0003-2643-8003
How to cite this article:
Kota SK, Shaik SA, Talukder R. Unsteady Shock Interaction Mechanism on a Double Wedge at Mach 9. *J Adv Res Aero Space Sci* 2020; 7(1&2): 1-14.

Date of Submission: 2019-12-02
Date of Acceptance: 2019-12-17

A B S T R A C T

Present computational study explores arrangement and association components of shock and boundary layer for low enthalpy Mach 9 progressions of nitrogen over twofold wedges, which have fixed fore and different rearward points of 30^0 and 45^0–60^0, separately. We utilize a thickness based limited volume Navier-Stokes solver to reproduce low enthalpy Mach 9 progressions of nitrogen over twofold wedges. The solver is first and second request precise in reality, separately. The lattices utilized in recreations of twodimensional laminar streams comprise of various squares of organized work. Depending on the power, impingement point, and impingement area of transmitted shock wave, the subsequent unfavorable weight slope related unsettling influences on the wedge surface can trigger complex stream material science both in subsonic and supersonic areas. We watch a solid communication between the twisting of the boundary layer and the bow shock just as the transmitted stun for high rearward points. Correlation of the gotten brings about terms of general flow material science shows that there exists a toward the back point limit an incentive for such communication which is in the scope of 45°–50^0.

Keywords: Hypersonics, Machnumber, Shockwave, Boundary Layer, Shock Interaction, Turbulence Models, Shock Wave Boundary Layer Interaction

Introduction

Unsteady interactions of shock waves take place when a blast wave impinges upon a building or an aircraft, when the shock wave generated by a sharp energy release in some installation (a laser-driven fusion plant, for example) hits the wall or when the shock waves generated by an exploding gas mixture interact in a channel. A much-studied case involving the interaction of shock waves with an obstacle occurs in the driver section of shock-driven wind tunnels of short running times.[5] The unsteady flow of hot gas through the nozzle generates shock waves and vortices. The starting conditions in such systems have a strong effect on their overall performance.

The unsteady interactions accompanying combustion and detonation processes in gases, are of particular import, since the complex wavefront systems resulting from such interactions arise due to the confluence of the shock waves and form the driving mechanism of steadily-propagating detonation fronts.Bazhenova et al.[1]

The primary difficulty in producing a satisfactory theoretical analysis of the problem lies in producing a solution to the partial differential equations describing the unsteady motion of a compressible viscous gas simultaneously with the equations describing the chemical kinetics. The flow to be considered in these problems is further complicated by the interaction of shock waves with the boundary layer, which gives rise to separated flow patterns. The major stress in such investigations has, therefore, been laid on experimental studies, usually conducted in shock tubes.[1]

The proper prediction of thermal and structural loads is crucial for the design offuture space transportation systems. Especially the thermal and structural loads caused by shock-shock interactions may pose sign cant restrictions on the overall system. Shock shock interactions are frequently found in supersonic and hypersonic low fields and are characterized by a wide range of relevant ow phenomena on deferent length scales. Pertinent examples of shock-shock interactions are the Edney type IV interaction as well as the less known Edney type VII interaction.

The Edney type IV interaction is frequently used in theoretical and experimental investigations as it leads to high aero-thermal loads on the body surface. Depending on the particular configuration, Edney type IV interactions may show unsteady phenomena.

Due to their high-frequencies, these unsteady mechanisms cannot be fully capturedin experiments. Therefore, highly-resolved CFD simulations are an essential means to investigate such configuration.

The Edney type VII interaction was observed for a nitrogen configuration reddened by Yamamoto et al.[7] The supersonic jet of this type of shock-shock interactionis strongly curved. Because of the large distance between the jet and the body surface, this shock interaction leads only to moderate thermal and structural loads. However,the shock structure itself is more complex than the Edney type IV interaction asmore shock interference patterns are observed.

The proper CFD simulation and prediction of the Edney type IV and type VII shock interaction patterns is a challenging task. The structure of the incident oblique shock wave and the main shock must be properly captured in order to predict the resulting shock patternshown by Sravan kumar et al.[6] These strong shocks are formed at a certain distance ahead of the vehicle surface and spread out over a larger area. In addition, the boundary layer and especiallythe wall temperature gradient need to be properly resolved in order to capture the wall heat flux and to predict the thermal loads on the vehicle surface. Strong interaction patterns, which are potentially unstable by Grasso et al.[9] can be found between the bow shock and the boundary layer. To account for the high-temperature low field behind the shock pattern, the physical modeling of the numerical simulation must account for chemical and thermal non-equilibrium effects.

Classification of Shock-Shock Interactions

Shock-shock interactions have been widely discussed in the literature over the pastdecades. Referring to Sanderson (1995)[10], the shock interference pattern depends on the strength and angle of the intersecting shocks, the geometry of the body around which the interference pattern is formed, the relative location of the impinging shock on the body and the gas properties, i.e., the ratio of special heats.

The most comprehensive classification of shock-shock interactions was carried out by Edney (1968), who experimentally and theoretically investigated the impingement of anoblique shock wave on a strong bow shock in front of a blunt body.

Edney distinguished six shock-interaction patterns named as type's I-VI. The particular type depends on the location of the impingement on the bow shock. The Edney type IV interaction is the most critical shock-shock interaction in terms of the aero-thermal loads on the wall (Grasso et al. 2003).[9] A detailed analysis of the front section of the shock interaction pattern was carried out for double-wedge geometries by Olejniczak et al. (1997).[11]

A supersonic jet forms between two triple points and reaches into the subsonic region behind the bow shock. The two bends upwards by a combination of several expansion and compression waves. The wall impingement of the two passing through the shock pattern of the jet and the terminating shock leads to high pressures and temperatures on the surface of the blunt body.[8] This configuration exhibits an unstable behaviour and is highly sensitive to the exact location of the shock impingement.[13] When the impinging shock wave is moved upward, the jet begins to bend upwards along the cylinder surface. This state is frequently characterized as a type IVa interaction (Grasso et al., 2003).[9]

For a high location of the impinging shock, Yamamoto et al. (1999)[7] experienced a newtype of shock-shock interference which involves a/ supersonic jet streaming towards the upper downstream without stagnating on the body".

This is in contrast to the type IVa interaction in which case the supersonic jet still touches the wall surface. Yamamoto et al. referred to this new interaction as type VII. The supersonic jet of this interaction is characterized by a strong vortices.

Unsteady Mechanism

The Edney type IV interaction is known as being inherently unstable. As explained in the following, different types of behavior are found in the literature which range from fully unsteady to steady ow characteristics of the jet structure.

No comprehensive systematic studies of the unsteady behaviour are known to the authors. However, the unsteady characteristics of particular configurations are subject to various publications: Referring to Lind & Lewis (1996),[3] the unsteadiness of the Edney type IV interaction depends strongly on the angle and strength of the oblique shock wave and its impingement location on the bow shock. They observed that small changes in the impinging shock properties may cause steady low fields to become unsteady.

Following the observation of Lind & Lewis (1996),[3] the high-frequency jet unsteadiness is seen to be related to the formation of a vortex near the junction of upper shear layer and the termination point of the supersonic jet, its breakdown and then its propagation along the upper portion ofthe cylinder, causing shear layers to be generated and then shed." The published plots of the peak pressure and the jet impingement angle for a particular configuration show a quite regular pattern with only minor variations in the magnitude over a longer period of time. This is in contrast to results of a slightly modified configuration with a lower angle of the oblique shock wave and a higher impingement location on the bow shock. In this case, only initial oscillations were discovered. These were strongly damped in time and resulted into a steady-state solution. This eject was also supported by a coarser girder resolution. by Furumoto et al. (1996).[12] also observed the unsteady characteristics of the Edney type IV interaction in their simulations of 5-species air in thermo chemical non-equilibrium. The investigated configuration resulted in stronger unsteady characteristics in the initial phase of the simulation. A sustained oscillation in the maximum surface pressure could be reached once all transients of the solution were damped out. Furumoto et al. concluded that the most stable solution was obtained with a shock impingement angle which leads toa shock-shock interaction in the transition regime between a type III and IV interaction.In case of more unstable solutions, / the largest degree of unsteadiness was the result ofalternating shed vortices both above and below the jet", which is similar to the mechanism described by Lind & Lewis (1996).[3] though the vortex sheddingon both sides of the jet seems to be inuential in the configuration of Furumoto et al. Observations of unsteady behaviour with deferent intensities are also reported by severalother authors, for example Yamamoto et al. (1999)[7] and Gaitonde (1993).[2]

Free Stream Conditions

Mach number 7.11

Stagnation enthalpy (MJ/ kg) 2.1

Static temperature (K) 191

Static pressure (kPa) 0.391

Velocity (m/ s) 1972

Density (kg/ m3) 0.0071

Unit Reynolds number 55 880

Test time (μs) 327

Result and Discussions

Shock Interaction Mechanism

At the point when a hypersonic stream over a twofold wedge is considered, the connection of stun waves can make complex temperamental streams and extreme warmth moves from the surface as detailed in number of numerical and test studies. Figure 1–4, for example, when the toward the back edge, θ2 is higher than the greatest diversion edge comparing to free stream Mach number, the two diagonal stuns that structure at the main edge and the pressure corner are joined by a withdrew bow stun. Contingent upon free stream Mach number and the wedge edges, extra stun wave/ s might be considered. While the time ward stream material science and the warmth move system are come about from time slack between the in viscid foundation times of the three stun waves previously mentioned above, insecure and progressively confounded communication components may occur because of detachment further more, reattachment of the limit layer on the wedge surfaces. At the point when a solid stun wave infiltrates into a limit layer on a divider, it makes antagonistic weight inclination which thickens the limit layer by causing a detachment bubble. Stun initiated division air pocket and created stream material science are portrayed in Figure 5. The limit layer at that point diminishes downstream of the impingement point. Thickening and diminishing limit layer produce pressure waves in the downstream of the impinging stun wave which may consolidation and structure a Reattachment Stun (RS) wave. As the division air pocket grows, a partition Ctun (SS) frames upstream of the impingement point. In expansion to the pressure waves, an extension fan frames between the two stun waves. At the point when a supersonic stream over a twofold wedge is considered, a division stun and a reattachment stun structure upstream and downstream of the partition bubble that happens in the pressure Corner (CC) (see Figure 6). An association that is like the stun actuated partition system delineated in Figure 5 happens on the second slope of the twofold wedge. Transmitted Stun (TS) wave that rises up out of cooperation purpose of driving edge stun (LS) and Bow Stun (BS) encroaches on the subsequent incline and incites a partition bubble not with standing the one Figure 5. Stun initiated partition on a surface. Figure 6. already framed at the CC. The communication purpose of LS, BS and TS is called Triple Point (TP), from where a contact irregularity (CD) likewise develops. In Secs. IV B–IV F, association systems and stream material science for the twofold wedge with fixed fore point of 30◦ and different toward the back edges of θ2 = 45◦, 50◦, 55◦ and 60◦ are clarified. The cases are assessed for interim of 0-327 μs which is the test term of the investigation of Swantek and Austin. For the lower estimations of toward the back points, for example, 40◦, rather than a BS a sideways stun happens and connects with the LS and SS and the stream turns out to be consistent toward the finish of the stun foundation time.

Interaction Mechanism for θ2 = 40°

compression corner shock is strengthened by merging compression waves. The separation and the reattachment (compression corner) shocks, which emanate from the first and the second ramps, respectively, merge before meeting the transmitted shock wave at instant of 30 µs.

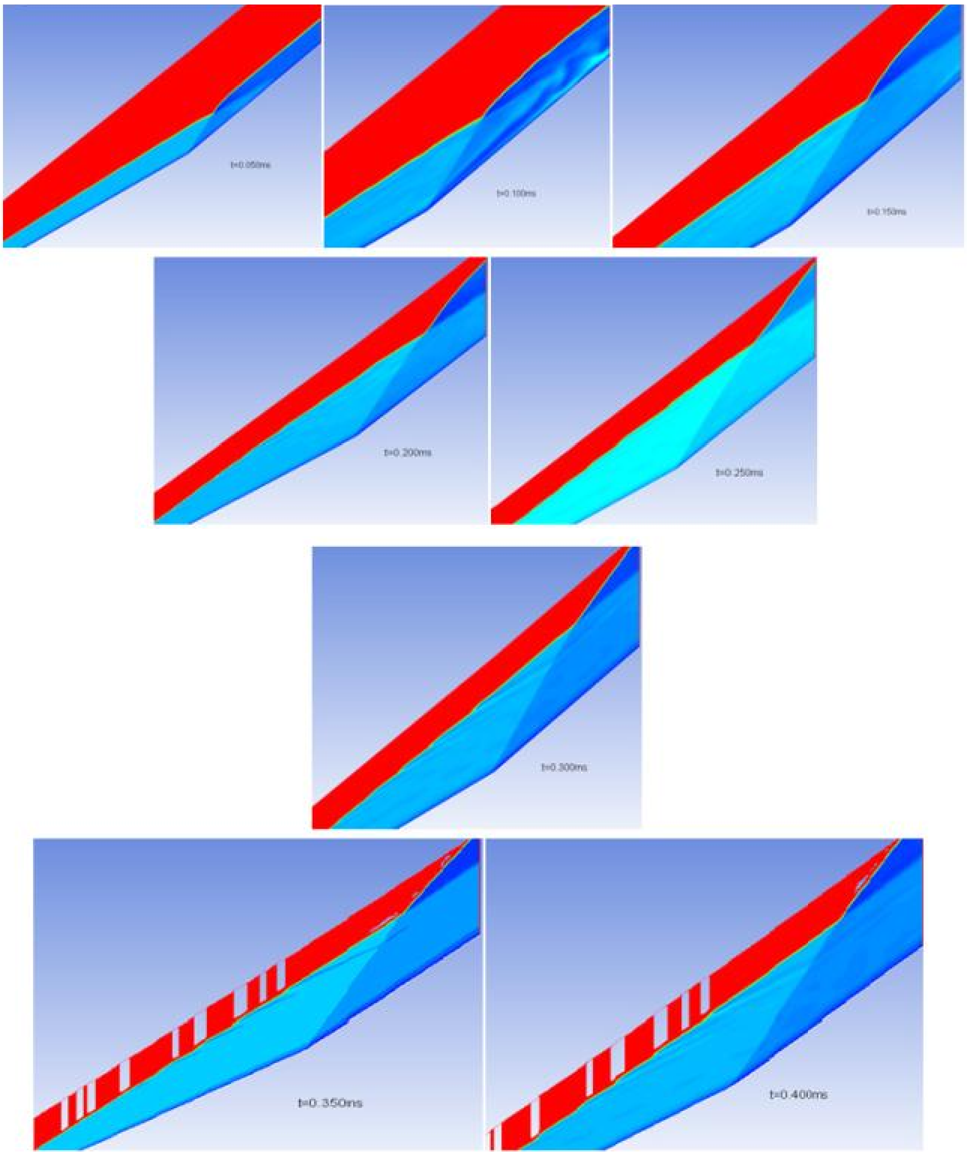

Figure 1

Interaction Mechanism for θ2 = 45°

In order to describe complex flow physics resulting from the interactions of the shock waves with boundary layer and other shock waves, instants of Pressure contour from 0 to 400 µs with an interval of 50 µs are shown in Figure 7. The ending time instant of 400µs is also included in Figure 7 to show that the flow almost reaches steady state. A contact discontinuity that separates the subsonic and supersonic flow regions is apparent at t = 30 µs. Sonic lines are depicted in the contour plots as white solid lines. As the separation bubble that forms on the CC grows, a SS forms and the

The merged and the transmitted shock waves refract after interacting with each other and the former extends to a point on the contact discontinuity. The direction of the contact discontinuity suddenly changes at this location because of increased pressure behind the shock wave and a convex corner forms, An expansion fan formed at the convex corner accelerates the flow.

As can be seen from the instant of 50 µs, the SS is significantly weak compared to the RS. Relatively weak, another reattachment shock, RSi appears downstream of the impingement point of the transmitted shock wave on the second ramp. A Separation Shock (SSi) that forms upstream of the TS impingement point is very weak because of a quite small separation bubble size of which is dictated by the impingement angle and strength of the TS. Comparison of the instants of 30 and 60 µs reveals that the LS become straighter as time pass by and thereby the location of the TP changes. As a consequence of the displacement, the impingement point of the TS on the second ramp and the RSi move towards the expansion corner. At the instant of 60 µs, the TS impinge send of the ramp, where an expansion fan has already formed. The flow above the corner as wellas the contact discontinuity bends towards the wedge surface under the influence of the expansionfan. The RSi disappears approximately at 60 µs. As can be seen from the first three instants, the T Scontinuously weakens.

Temporal variations of normalized pressure values at three points that are located behind the final positions of LS, BS and RS are shown in Figure 8. The locations of the three points are given in Table 2. The instants of the sudden jumps in the variations are interpreted as the establishment times, the values of which are also given in Table 2. As can be seen from the figure, the three shock waves can be ordered in terms of their in viscid establishment time from the longest to the shortest as the BS, the LS and the RS, respectively. As the separation bubble formed on the CC grows, the SS moves towards the leading edge (see instants of Mach contours at t = 30, 60 and 90 µs). As a result of the movement, the pressure behind the SS and RS continuously varies. Although the SS continues to move towards leading edge, the flow becomes steady later.

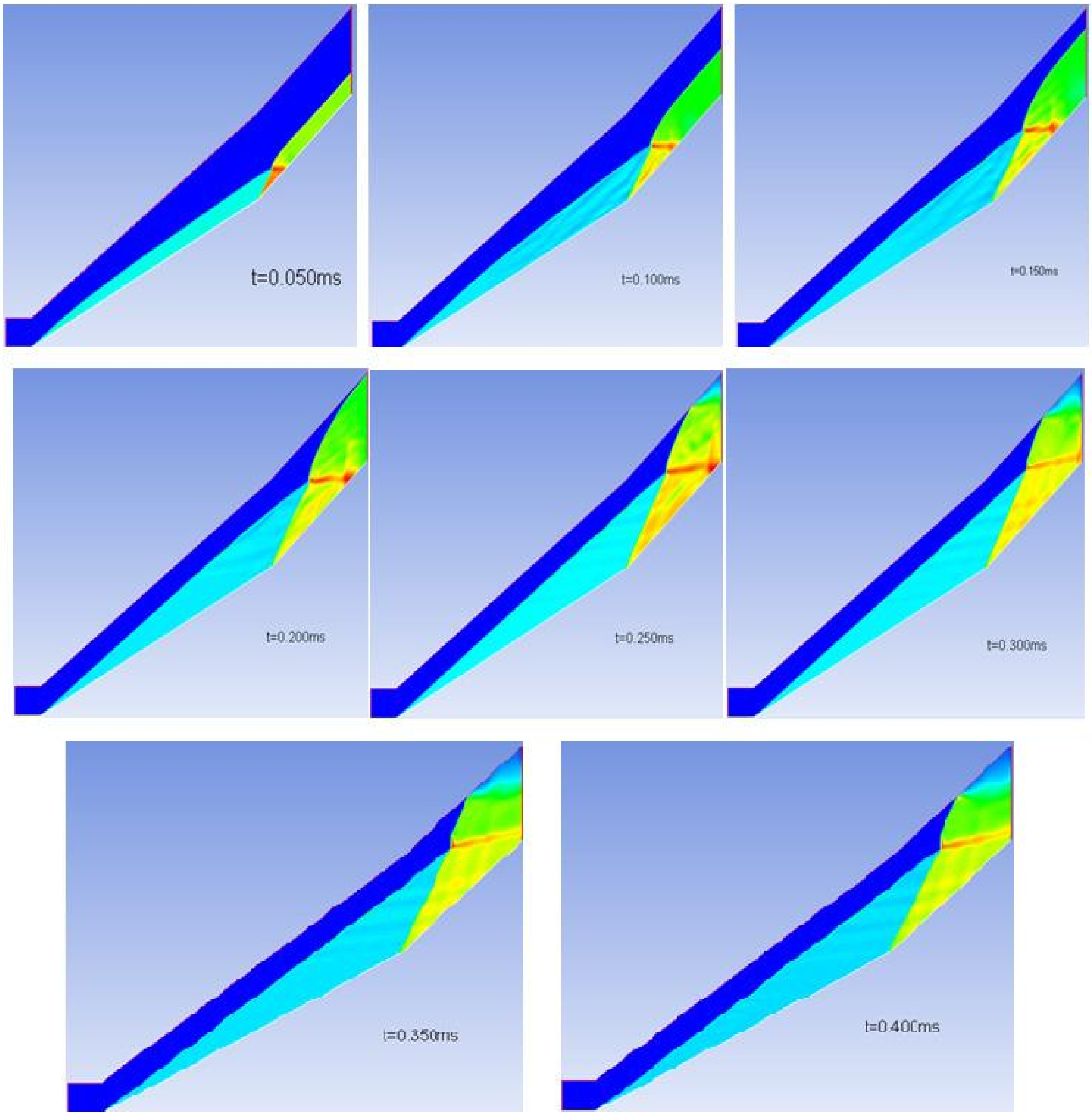

Figure 2

Interaction Mechanism for θ2 = 50°

Mach contour plot instants of the flow are shown in Figure 9. An interaction mechanism that is very similar to the one depicted in Figure 6 is observed for this case from 0 to 60 µs. SS and RS form upstream and downstream of the separation bubble as observed in the case of θ2 = 45◦. Eventhough the flow physics is quite similar, the strength of the two shocks and the distance between them are higher for θ2 = 50◦. The interaction mechanism starts to differ from the previous caseespecially in the vicinity of CC, when the influence of the TS impingement point becomes eminentas explained below.

As observed in the previous case, another separation bubble forms at the impingement point of TS on the second surface of the wedge. The TS is relatively stronger and separation bubble is bigger compared to the previous case. Although the RSi is visible from the beginning of the Mach contourplots in Figure 9, there is no SSi prior to 80 µs.

The impingement point of TS on the second wedge moves in the downstream direction from 0 to 80 µs, when the LS and RS continue to become straighter. As the impingement point moves in the flow direction, the size of the separation bubble and the length of the separated flow increase.

During the movement of the TS impingement point towards the expansion corner, SSi and RSi are relatively weak and thereby the directional change of the contact discontinuity at the impingement points of the two shocks is so small.

The separation bubble and BS continue to grow and get stronger beyond 80 µs. Since LS and RS have already reached their establishment time, growing BS causes the impingement point move to wards CC. As a result, the angle of TS with respect to the wedge surface increases during themotion. Increased angle affects the shape and size of the separation bubble, which causes formationof a SS during the motion towards CC (see Mach contours in Figure 9). The movement continues tillthe two separated

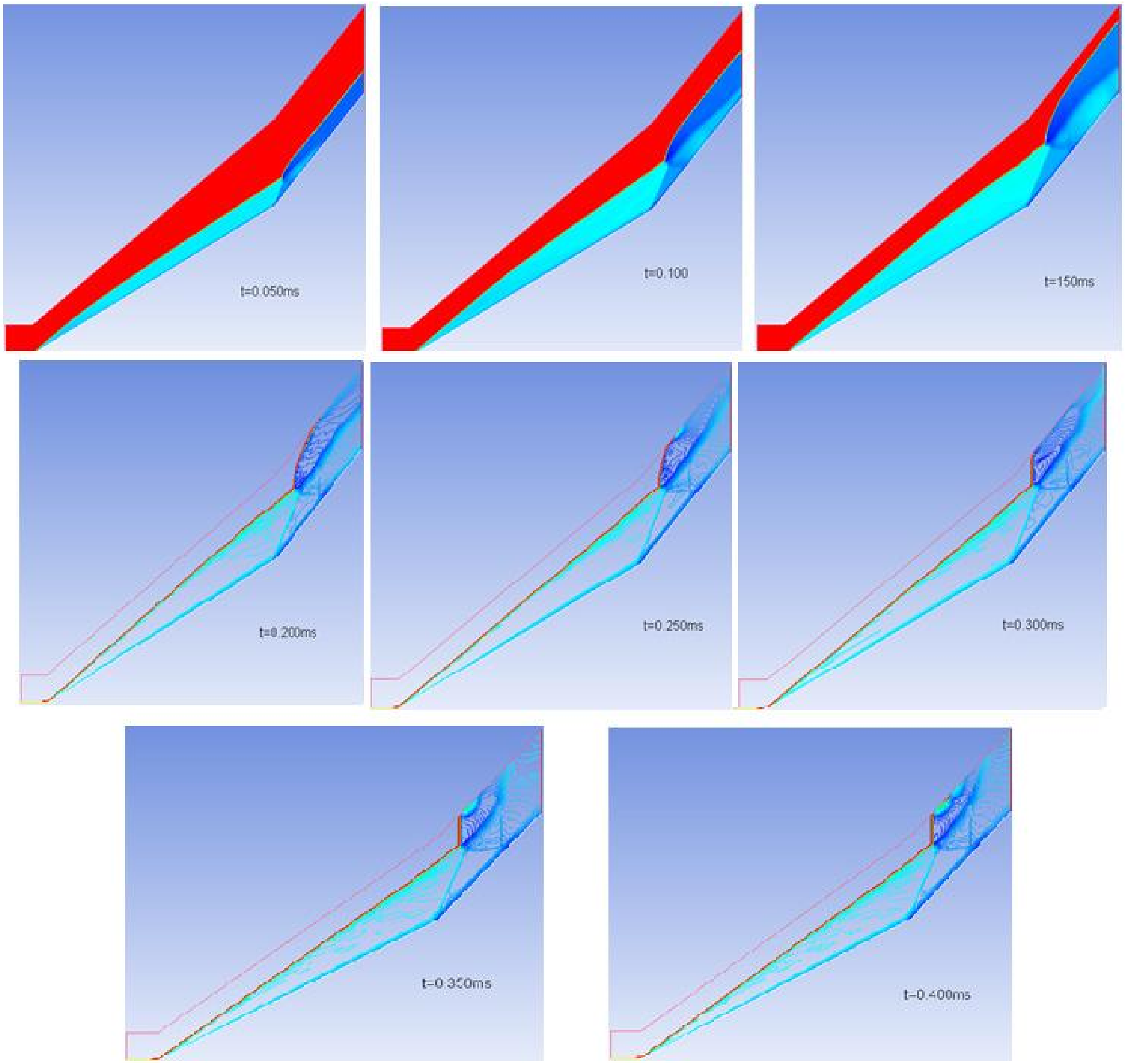

Figure 3

flows come in contact, approximately at 185 µs. From 80 to 185 µs, SSi and RSi get stronger. SSi and RSi are quite stronger during their motion towards CC than the one to wards expansion corner. The two shock waves are strong enough to change the direction of the CD at their interaction point with it. As a result of the interaction, two convex corners form in the supersonicregion which create expansion fans. The two expansion fans and the deformation of the CD becomevisible in Mach contour plot starting from instants of 120 µs.

SSi and RS merge in the vicinity of CC at t = 185 µs. After the merge, the separated shear layer starts to extend towards Leading Edge (LE) which causes SS to move upstream. The triple point alsocontinues to move upstream during the movement of SS. The change in the emerging point of SS affects its impingement point on CD. As the impingement point moves towards TP, CD bends awayfrom the surface. This mechanism ends when the impingement point reaches to TP. Beyond this instant, CD emerges from the interaction point of SS, LS and BS. When RS and SSi merge at approximately at 185 µs, increased adverse pressure gradient makesprimary separation bubble formed in the compression corner to grow substantially in the directionof the wall normal. The flow underneath the bubble accelerates and generates a supersonic stream(see t = 210 µs in Figure 9). The shear layer deforms and additional shock waves occur in the flow field due to the growing bubble. The fast growing bubble causes separation point, as well as SS to move towards the leading edge. Another separation shock takes place upstream of CC which is not visible in the Mach contours.

Beyond 250 µs, SS starts to interact with LS and they refract. While the refracted SS intersects with BS, the refracted LS interacts with TS that emerges from the interaction point of refracted SS and BS. The interaction point of refracted SS, BS and TS now becomes a primary TP, which isdefined as the interaction point of BS with another shock. A flow field that is bounded by CD andthe sonic line of the boundary layer on the wedge surfaces is supersonic from 0 to 327 µs.

Interaction mechanism for θ2 = 55°

It is obvious that increased aft angle generates stronger BS with longer stand-off distance. 27 Since there is no change in the strength of the LS, the increased intensity of the BS results inrelatively stronger TS emanating from the TP. TP, CD and TS are visible at instant of t = 30 µs in Figure 10 as observed in the previous two cases. However, RS and TS do not interact directly atthis angle, instead a Mach Stem (MS) forms between and connects them. Therefore, two new triplepoints, TP1 and TP2, form at the two ends of the MS.

Figure 11, depicts the new interaction mechanism and new shock waves. Two new shock waves, TS1 and TS2, which emerge from TP1 and TP2 impinge on the CD and the surface of thesecond wedge, respectively. TS1 and TS2 generate interaction mechanisms that are similar to theme chanisms generated by the refracted RS and TS in the previous cases, respectively (see Figure 6). A diamond shaped subsonic pocket takes place downstream of the MS, TS1 and TS2. Although the flow is subsonic behind TS1 after t = 40 µs, downstream of TS2 becomes fully subsonic at instant of 90 µs. The shock interaction mechanism creates a converging-diverging flow field confined betweenCD and the sonic line above the second wedge. The bounded region creates a decelerating and accelerating flow field which becomes supersonic behind the subsonic pocket again. LS, RS and BS get stronger from 0 to 60 µs as observed in previous two cases. The increasesin strength of former two shocks are dominant which cause the TP1 and TP2 to move in downstream direction. As a result of this movement, the impingement point of TS2 on the second wedge surface moves towards expansion corner as depicted in Figure 11 which is similar to the behavior of the TSat the lower angle cases. At instant of 60 µs, the primary TP starts to move upstream direction. Thisbehavior might be resulted from thickening boundary layer in the vicinity of the impingement pointof TS2. Increased deflection angle, which is the inclined boundary layer plus the second surface angle here, increases stand-off distance of BS.27 Compared to the other two cases, SSi is quite weak.

This weak shock wave merges with RS at the instant of 100 µs. Then, SS starts to move towardsthe leading edge because of fast growing separation bubble as observed in the case of θ2 = 50◦. Asupersonic stream appears in the boundary layer in the vicinity of CC at instant of 105 µs. Duringthe movement of SS towards the leading edge, relatively weak another separation shock takes place over the first surface due to thickening boundary layer. SS impinges on TP1 approximately at100 µs. The overall interaction mechanism depicted in Figure 11 remains the same till SS starts tointeract with TS at instant of 110 µs. Later, SS and TS intersect at a point that is located between the primary TP and TP1.

At instant of 140 µs, the shear layer that extends from the separation point to the impingement point of TS becomes quite straight. The supersonic stream under the shear layer also elongates. Asthe shear layer becomes straighter, RS becomes weaker and parallel to it that makes the subsonicpocket completely disappear at t = 140 µs. The interaction mechanism of TS and SS is very similarto the one of TS and RS for θ2 = 50◦. RS and RSi merge and impinge on CD. Downstream of themerged shock becomes subsonic in the vicinity of impingement point. The new subsonic pocketextends and later reaches the boundary layer on the second wedge surface at instant of 150 µs. When the impingement point of SS reaches the primary TP location approximately at the instant of 180 μs, the total number of SS waves generated by thickening boundary layer on thefirst wedge surface becomes two. After 180 μs, SS starts to interact with LS and refracts (see Figure 12). While the refracted SS extends to BS, the refracted LS interacts with TS that emerges from the interaction point of the refracted SS and BS. The interaction point of refracted SS, BS,and TS becomes now primary TP. This interaction mechanism is also similar to the one observedin the case of θ2 = 50◦. The shape of the supersonic flow field, which is confined with CD andthe subsonic portion of the boundary layers formed on the wedge surfaces, changes in time. This change might be resulted from the interaction of growing and moving separation bubbles inside the boundary layer. The flow mechanism inside the boundary layer is quite complex beyond180 μs where several supersonic stream and separation bubbles form. The thickness of the subsonicpocket that appears inside the confined supersonic flow field changes as the shape of the boundarylayer and contact discontinuity varies. The good agreement between our Mach contours andRef. 9 at t = 260 μs proves that the earlier stages of the mechanisms described here are also verysimilar.

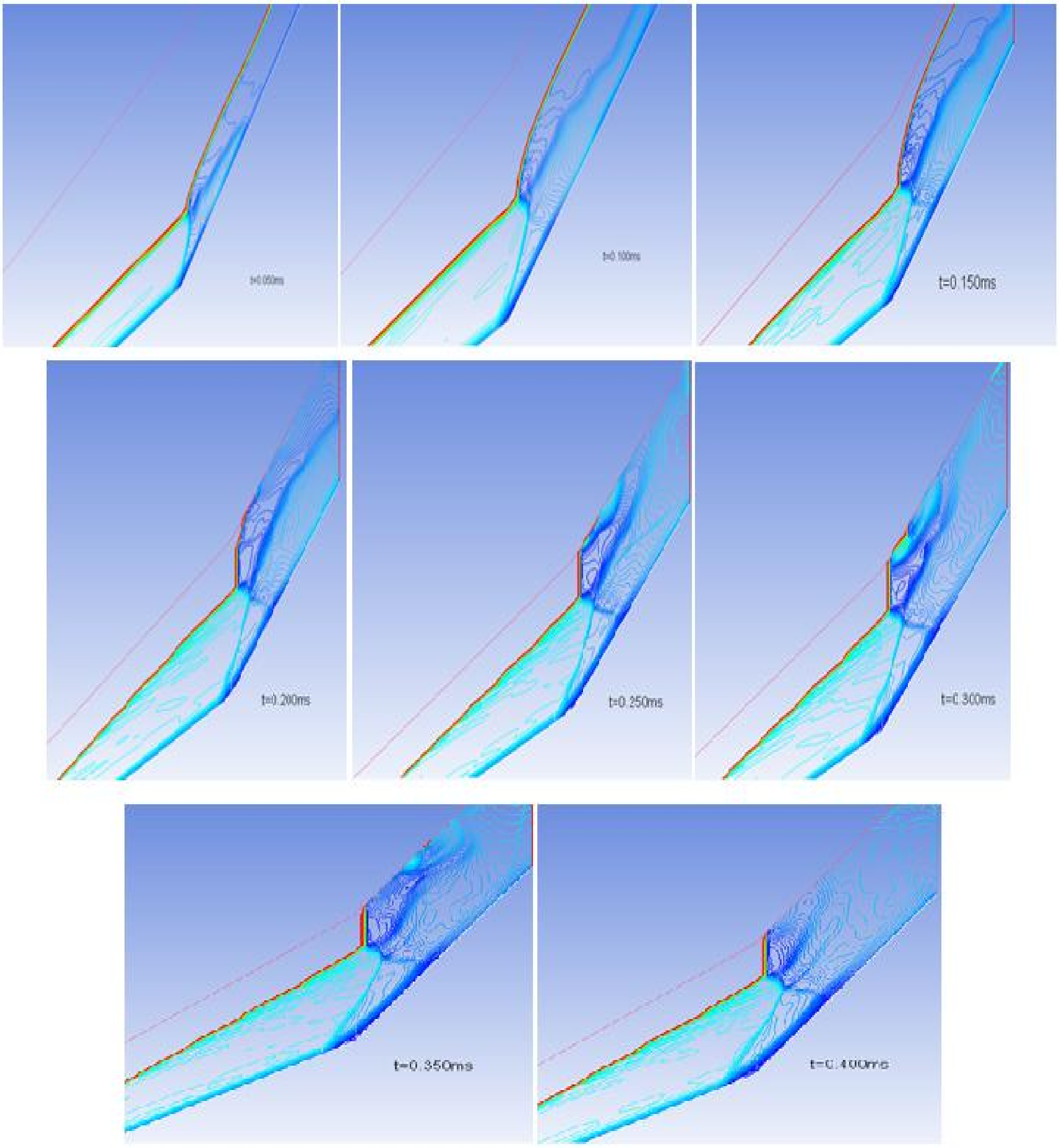

Figure 4

Interaction mechanism for $\theta2 = 60^\circ$

General physics and interaction mechanisms of the flow are quite similar to those of $\theta2 = 55^\circ$ (see Figure 11). The interaction mechanism, Edney Type V can be seen from the Mach contour Snapshot at instant of 30 µs shown in Figure 13.

As expected, increased deflection angle makes BS stronger and the subsonic area behind it wider. It is obvious that this discrepancy also affects the intensities of the resulting shocks, such as MS and TS. Other discrepancies in the instants of the interaction stages of $\theta2 = 55^\circ$ and 60° areexplained below.

From 0 to 60 µs, the impingement point of TS2 on the second surface moves towards the ECand then stops. Up to 45 µs, there is only Edney Type V interaction where the lower triple point is formed by the Mach stem, the merged SS and RS and TS2. Beyond this time SS starts to move to wards the LE and it impinges on the Mach stem. At the instant of 75 µs, SS impinges on the uppertriple point. Up to this time, primary triple point continues to move upstream direction. The lengthof MS is significantly longer for the case with $\theta2 = 60^\circ$ than 55° at all instants. The subsonic pocketbehind MS disappears earlier for the present case at t = 90 µs. Before SS impinges on the primarytriple point at t = 140 µs, several supersonic stream and vortices with high

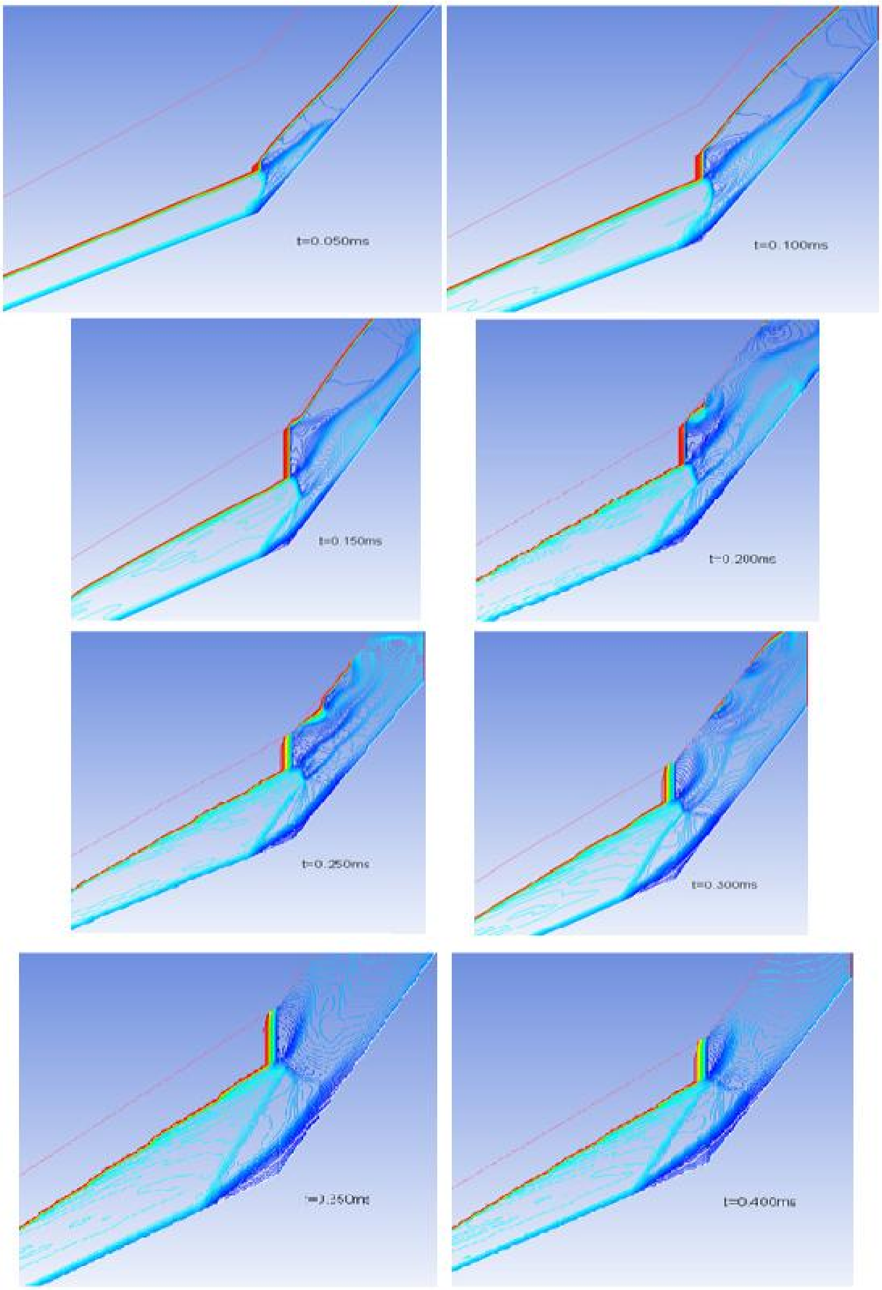

Figure 5

intensities appear insidethe boundary layer (see instant of 100 μs). Beyond 140 μs, the interaction mechanism shownin Figure 12 is observed. Dynamics and formation of bubbles, coalescence and displacement ofsupersonic streams taking place inside the boundary layer create complex interaction mechanismsin both subsonic and supersonic flow regions for θ2 = 60◦. In order to show unsteady nature of theshock interaction mechanism and the shear layers, the last two Mach contour snapshots are given in Figure 13.

Conclusion

We have investigated unsteady shock interaction mechanism for timestep variation of 50 μs from 0.050 μs to 0.400 μs, along with that successfully captured the flow phenomena, shock waves, shock fans, Jet structure, shock bubble during turbulence on the wall at the distance of 0.3 meters. The interaction takes place in the first quarter part of second wedge, and the intensity of interaction is fierce. We have procured the flow unsteadiness, vorticity and pressure waves in the entire flow field. Whimsically, the maximum pressure co-efficient has obtained in between 4.4 and 5.3 meters, and the maximum pressure co-efficient captured is 4.8.Therefore, the mach number falls to the transonic range inside the shock bubble, also often times it has reached to null with reverse flow. Immediately from the re-attachment point the friction has been attaining in every case, nevertheless, it reaches to maximum in between the range of 0.02 to 0.04.

T=0.050ms

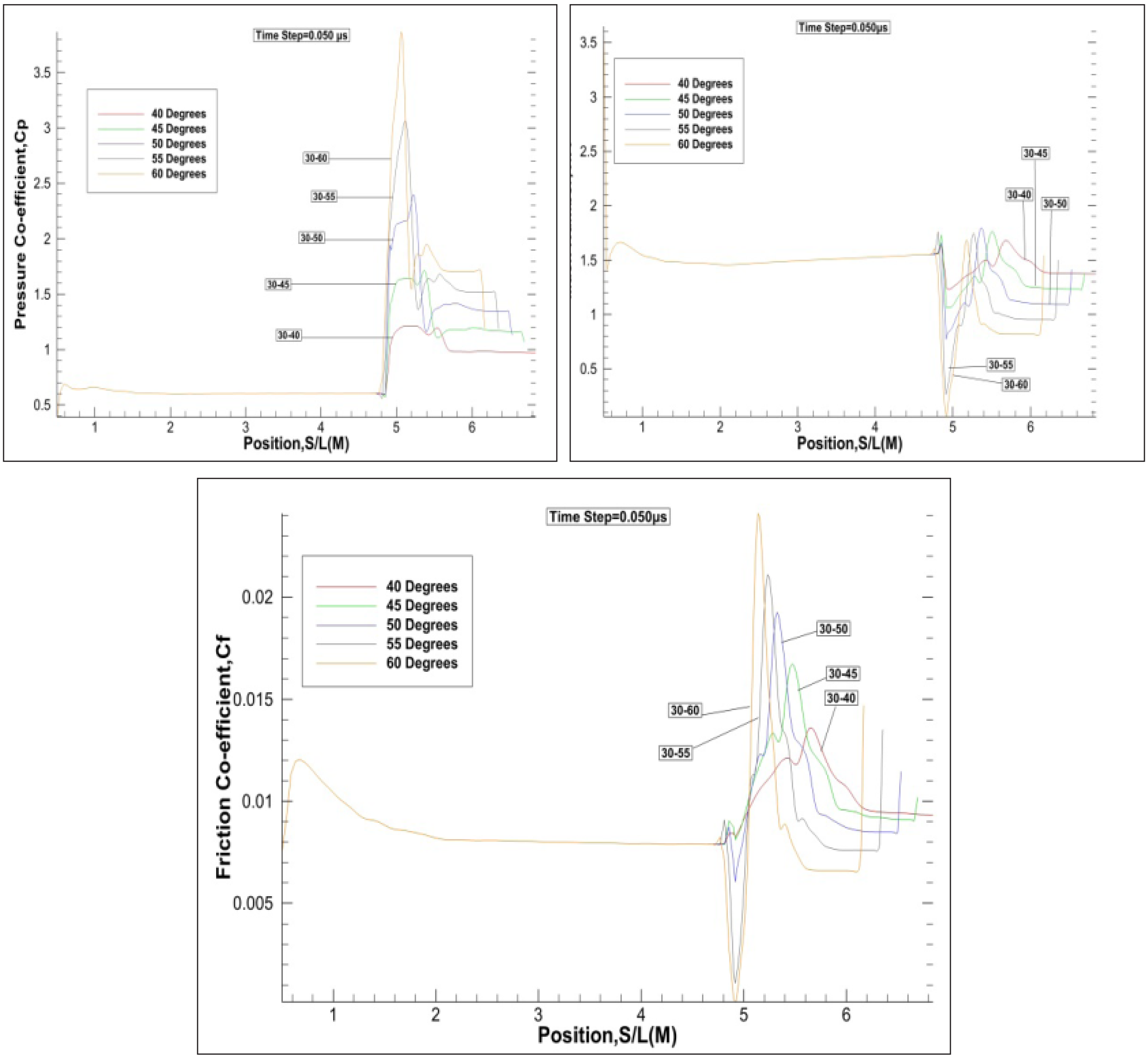

Figure 6

T=0.100ms

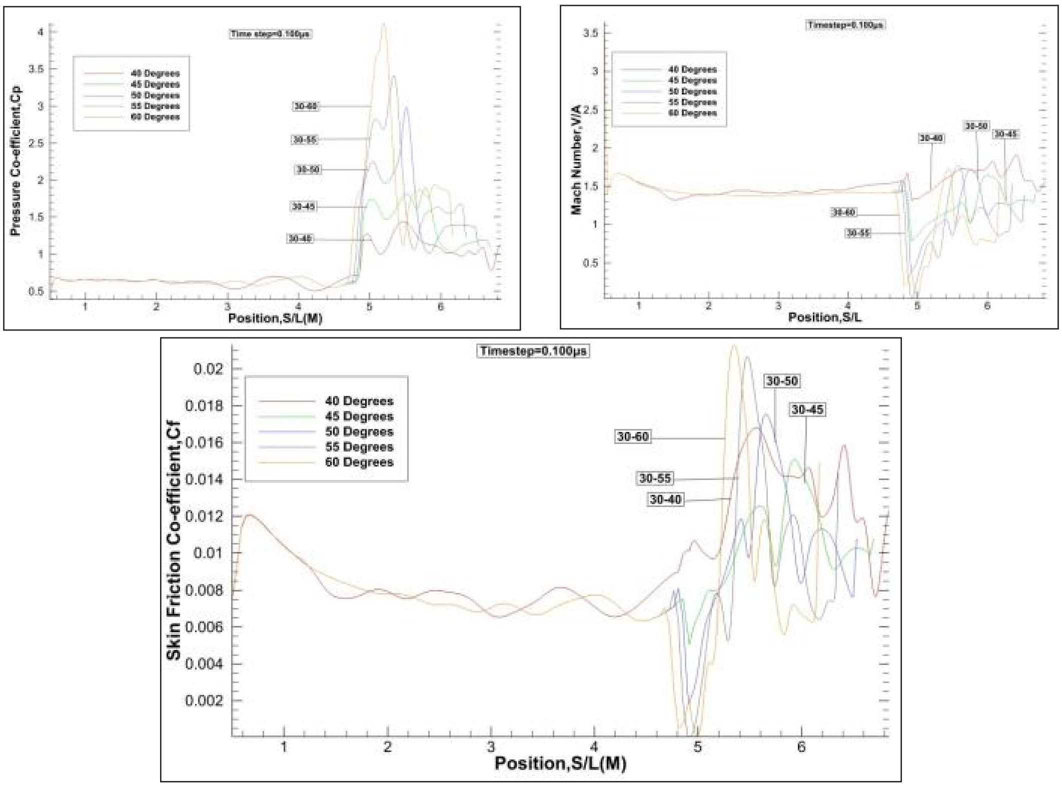

Figure 7

T=0.150ms

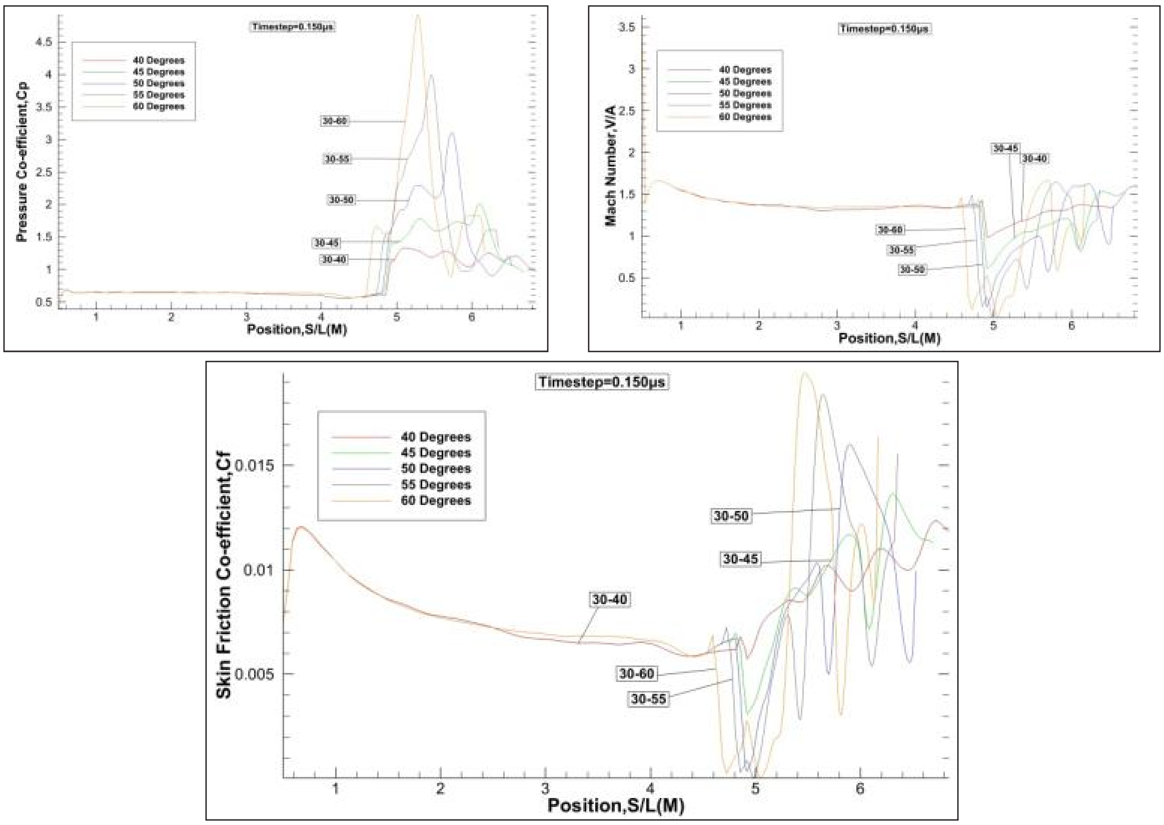

Figure 8

T=0.200ms

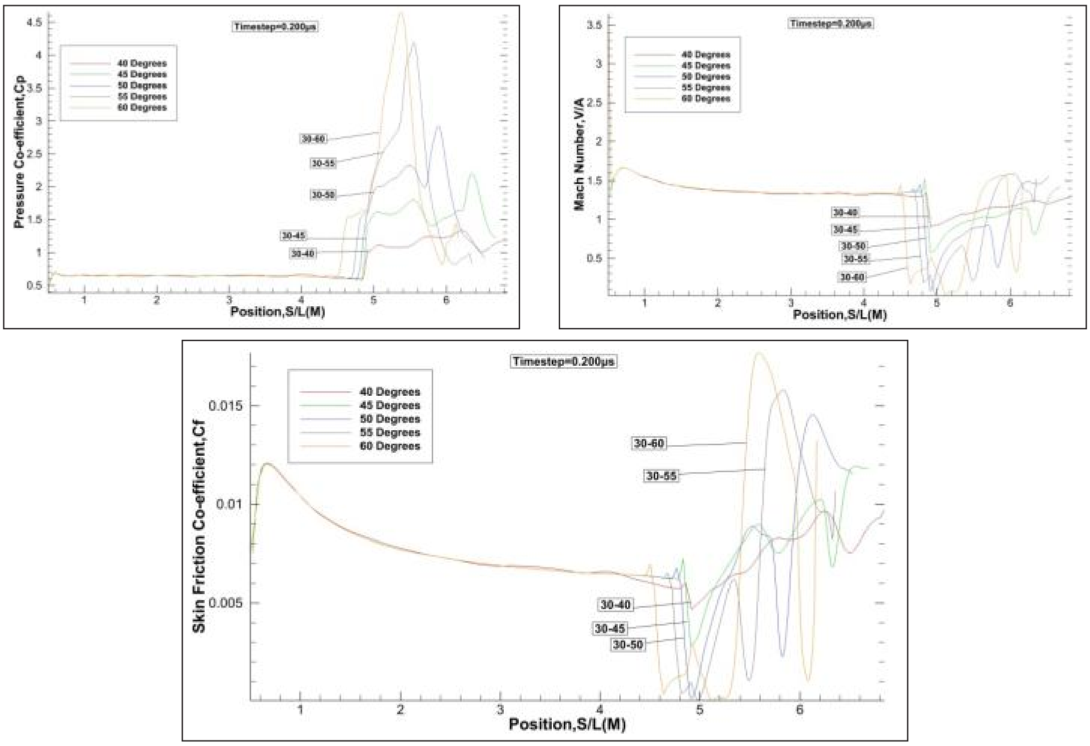

Figure 9

T=0.250ms

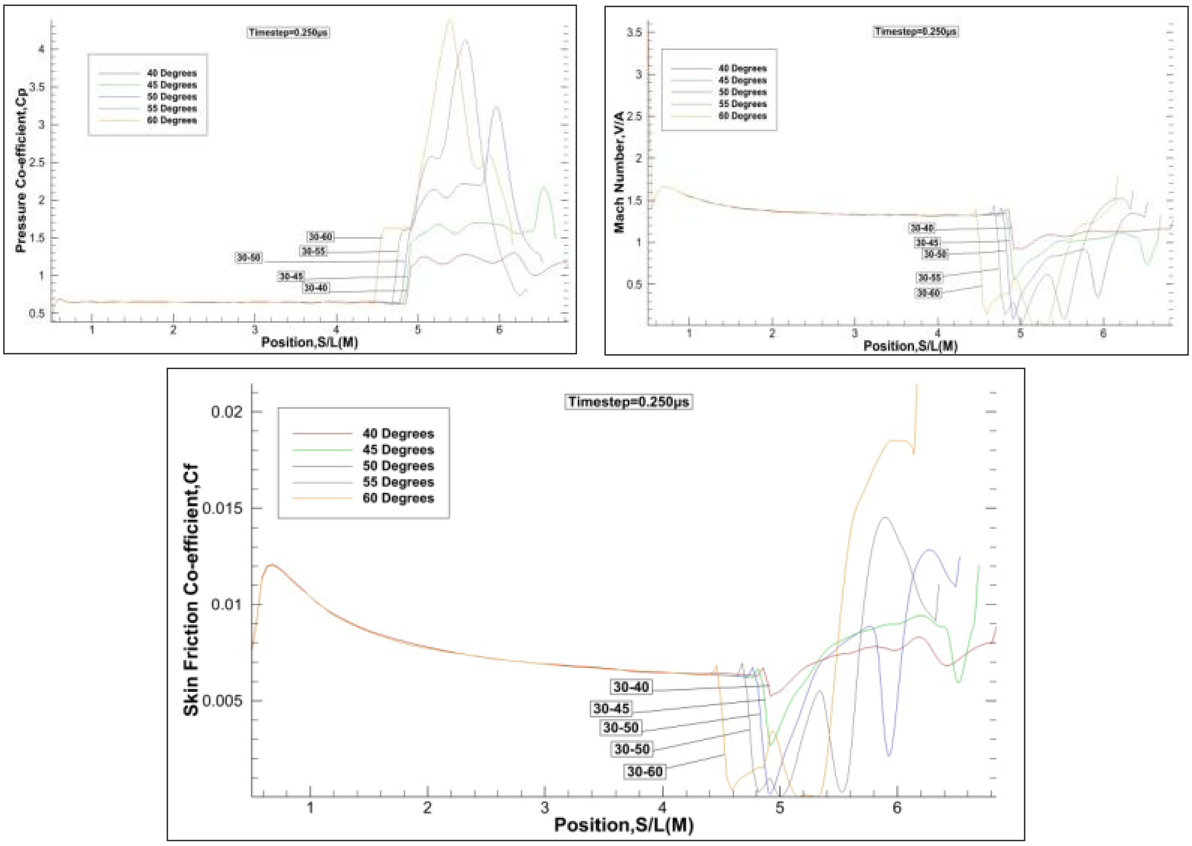

Figure 10

T=0.300ms

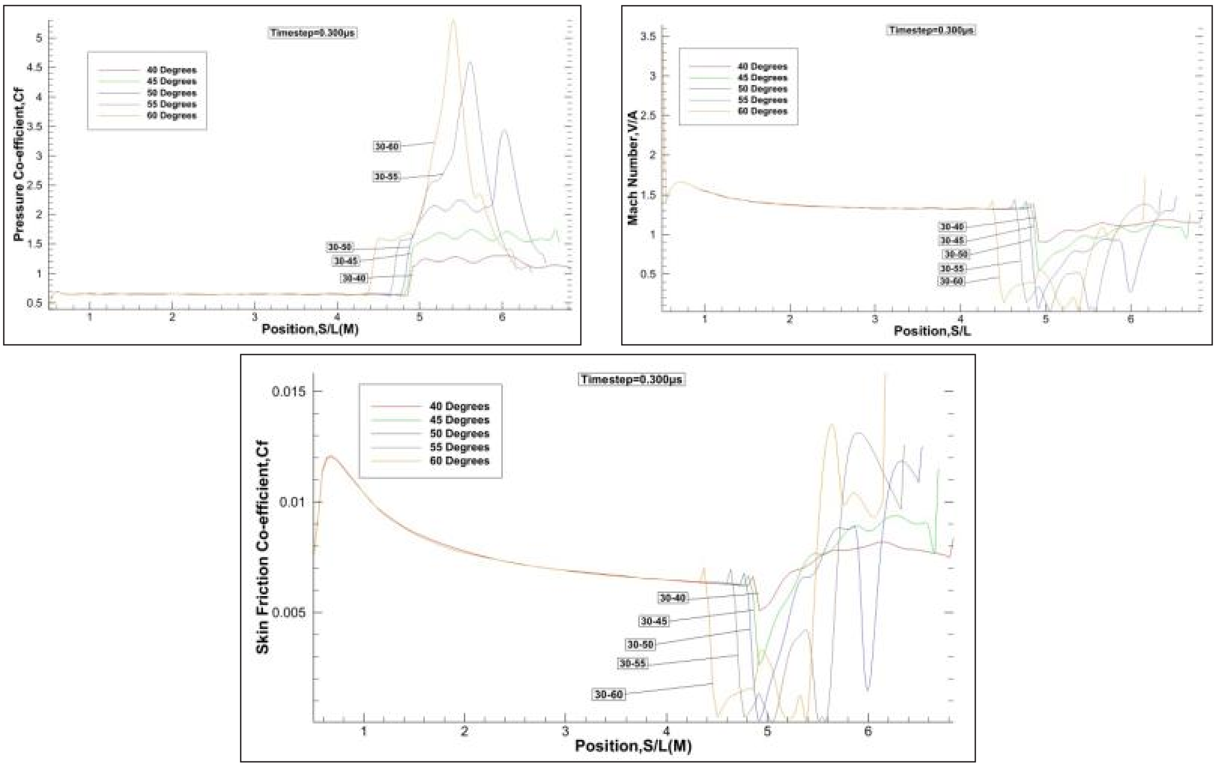

Figure 11

T=0.350ms

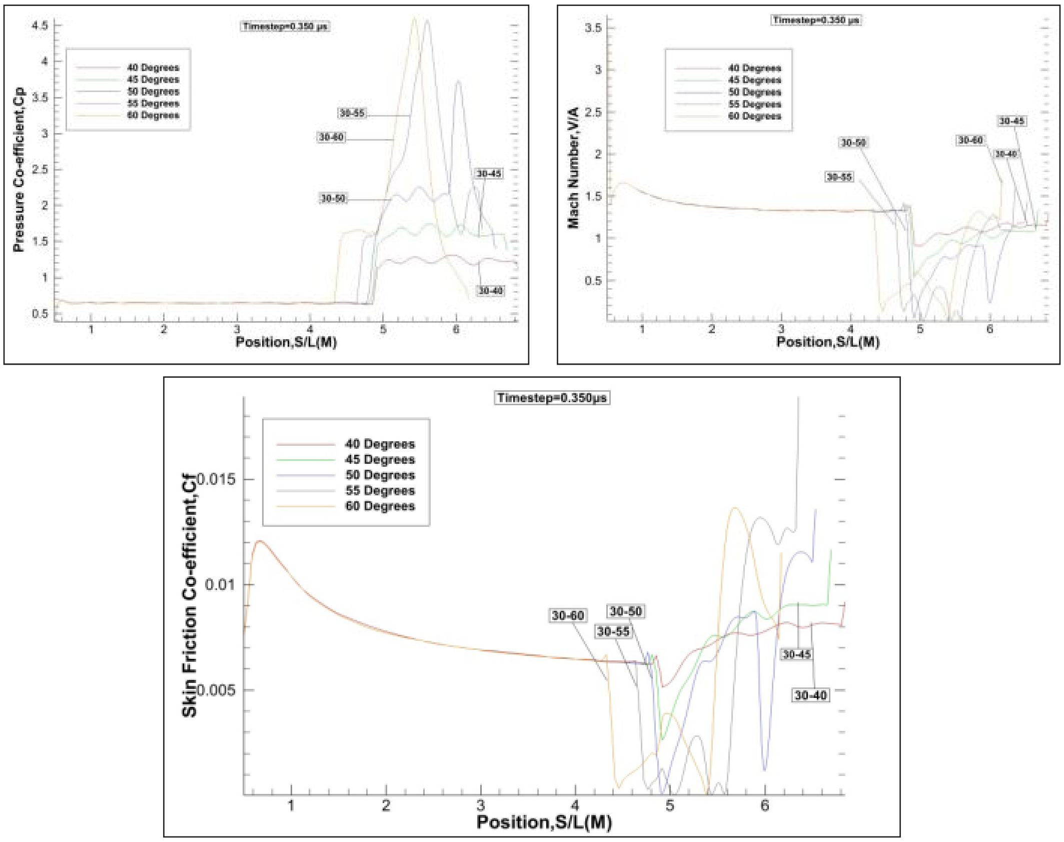

Figure 12

T=0.400ms

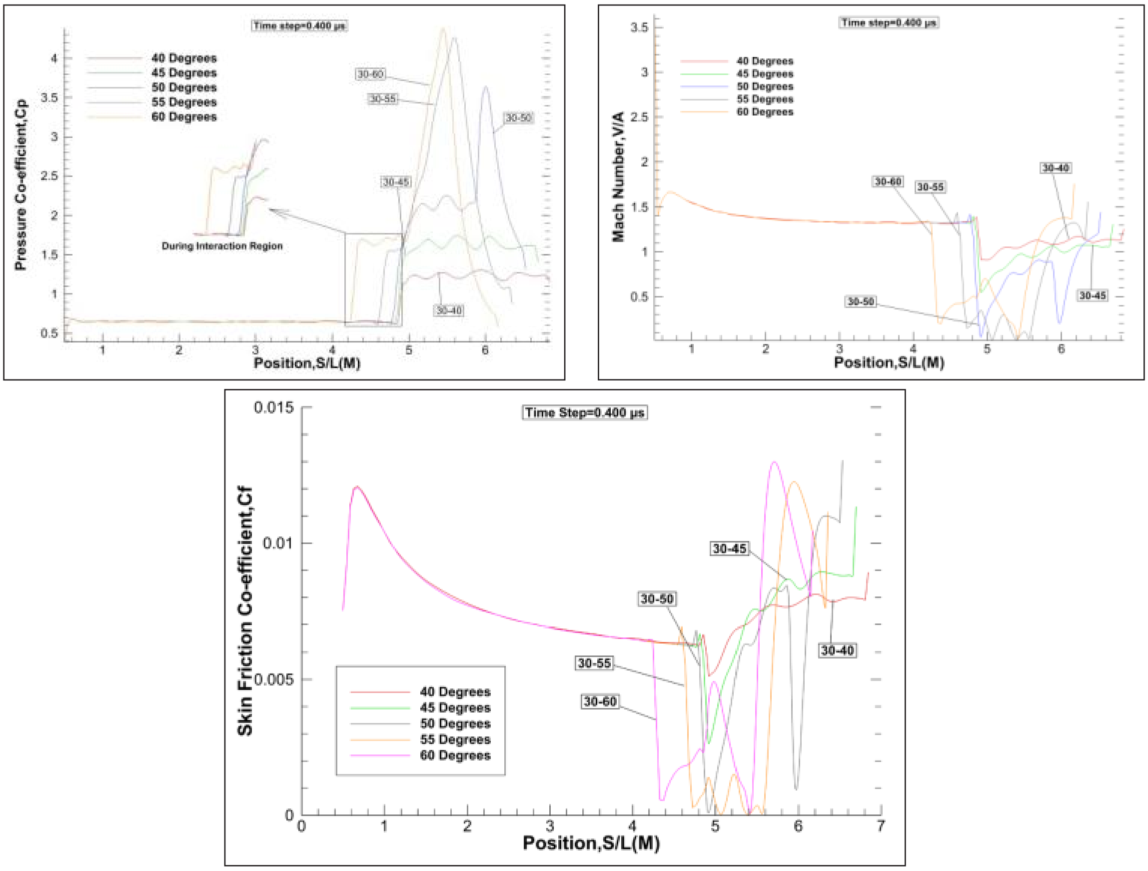

Figure 13

References

1. Bazhenova TV, Gvozdeva LG, Nettleton MA. Unsteady Interactions of Shock Waves. *Progress in Aerospace Science* 1984; 21: 249-331.
2. Windisch C, Reinartz B, Muller S. Investigation of the unsteady Edney type IV and VII shock-shock interaction. 2006; 24(6): 1-31,
3. Lind CA, Lewis MJ. Unsteady Characteristics of a Hypersonic Type IV Shock Interaction. *Journal of Aircraft* 1995; 32(6).
4. Barry E. Edney Effects of Shock Impingement on the Heat Transferaround blunt Bodies. *Aiaa Journal* 1968: 15-21.
5. Babinsky H, Harvey JK. Shock Wave-Boundary Layer Interactions. Cambridge University series. 2011; 373-383.
6. Kota SK, Shahid M. Linear and Non-Linear Turbulence Models of shock/boundary-layer interaction at Hypersonic Flows. *International Journal of Scientific Research in Physics and Applied Sciences* 7(5). ISSN: 2348-3423.
7. Yamamoto S, Takasu N, Nagatomo H. Numerical investigation of shock/vortex interaction in hypersonic thermochemical nonequilibrium flow. *Journal of Spacecraft and Rockets* 1999; 36: 240–246.
8. Kota SK, Shaik SA. (C.E.O). Navier-Strokes Computations on type-IVr shock–shock Interaction Mechanism Over Double Wedge(15-60) at High Speed Flows. *I-Managers Journal of Mechanical Engineering* 1999; 9(5). ISSN: 2230-9055(P), ISSN: 2249-0744(O).
9. Grasso F, Purpura C, Chanetz B et al. Type III and type IV shock/shock interferences: theoretical and experimental aspects. *Aerospace Science and Technology* 2003; 7: 93–106.
10. Sanderson SR. Shock Wave Interaction in Hypervelocity Flow. GALCIT, California Institute of Technology: PhD Thesis. 1995.
11. Olejniczak J, Wright MJ, Candler GV. Numerical study of inviscid shock interactions on double-wedge geometries. *Journal of Fluid Mechanics* 1997; 352: 1-25.
12. Furumoto GH, Zhong X, Skiba JC. Unsteady shock-wave reflection and interaction in viscous flow with thermal and chemical nonequilibrium. 34th AIAA Aerospace Sciences Meeeting and Exhibit, AIAA 96-0107.
13. Kota SK, Subbaraju PV(Ph.D). Numerical Analysis of Oblique Impinge shock-wave/turbulent boundary-layer interaction Using Reynolds Average Navier Stroke Equations. *Research & Reviews: Journal of Space Science & Technology (RRJoSST)* ISSN: 2321–6506, eISSN: 2321–2837.